)

SPECTRAL PROPERTIES OF THE STAR HD 141569A IN THE OPTICAL RANGE

H. N. Adigozalzade [a*], ***U. Z. Bashirova*** [a], ***N. Z. Ismailov*** [a],
S. A. Alishov [a], ***A. Z. Aghayeva*** [a], ***A. A. Aghayeva*** [b]

[a] *N.Tusi Shamakhy Astrophysical Observatory of Azerbaijan National Academy of Sciences, Shamakhy, Azerbaijan*

[b] *Baku State University*

In this work, the results of homogeneous spectral observations of HD 141569 of the Herbig Ae type star conducted at the Shamakhy Astrophysical Observatory in 2017-2018 are presented. It was shown for the first time that the spectrophotometric parameters of emission lines show both short-term (days) and long-term (years) variations. The reason for the variability in the emission spectrum in the optical range can be explained by the stellar wind and disk accretion. Based on the obtained spectral characteristics, it is shown that the star belongs to the class of β Pic-type fragmented protoplanetary debris disk stars.

Key words: Pre-main sequence stars – circumstellar disks – star formation – HD141569.

1. INTRODUCTION

The formation and evolution of young stellar protoplanetary disks is closely related to the processes of planet formation. The physical properties of the outer parts of such discs have been studied in recent years in scattered light images taken with large telescopes [1] and at the ALMA complex of sub-millimetre radio telescope [2]. These studies have shown that the sizes of rings, gaps, and asymmetric structures in disks reach several hundred au [3,4]. In the inner layers, signs of gas accretion, stellar wind, matter flow and dust sublimation are visible. All these processes lead to the formation of planets at a distance of a few au and their migration over millions of years. All these processes can be indirectly studied by

)AJAz:2023_2_43.pdf
* E-mail: hadigozalzade@gmail.com

http://doi.org/10.59849/2078-4163.2023.2.43

spectral observations. Although a statistically large number of young stellar discs have been studied so far, it is very important to continue research in this direction. For example, unusual systems such as HD141569 due to their evolutionary sequence warrant further study. The mechanism of formation of hydrogen lines in the star-disk system in this star remains unclear.

The spectral class of Herbig AeBe type star HD141569 is classified as B9-A0 [5], temperature 9750 ± 250 K, age 7.2 ± 0.02Myr, luminosity $16.6 \pm 1.07 L_{\odot}$ [6] and $27.0 \pm 3.6 L_{\odot}$ [7], with a mass of $2.14 \pm 0.01 M_{\odot}$ and a Gaia distance of 110 ± 1pc [8]. The star has a nonigniting disk system, shows a weak emission excess in the near-IR region, and is classified as type II according to the spectral energy distribution (SED) curve [9]. According to the results obtained in recent years, the protoplanetary disc formed around the star has a very complex structure and consists of separate arms distributed at different distances [10, 11]. At the same time, there is very little information about the internal structure of the disk. The study of the SED curve shows that the energy distribution in the near-IR region can be attributed to a normal photosphere, while the outer parts of the disk are already fragmented and the process of planet formation is proceeding rapidly [12]. An evolution scheme based on the amount of IR excess is proposed and this star is shown to be close to β Pic and α Lyr type [13].

Peristellar gas is observed in both atomic and molecular form, indicating that the disc has not yet reached the gas-rich fragmented disc stage. [14] and [15] showed that hydrogen lines do not show short-term variability.

Gahm et al. [16] showed that the Hα and Hβ lines in the spectrum of HD141569 show an emission profile, only the Hδ line is relatively clean. According to the initial classification criteria of Herbig [17], HAeBe stars are closely associated with gas-dust nebulae, with hydrogen lines showing a strong emission profile. Later, The et al. [18] added to these criteria the presence of emission excess in the near and far IR region. HD141569 shows an emission excess in the $12 - 100 \mu$m range, but it is not associated with any bright nebula. In 1938 Rossiger [19] proposed the star HD141569 as a potential triple system. The second component B is 7.5 arcsec from the center A, and the third component C is 1.5arcsec. Gahm et al. [16] assigned the spectral class of the component as G0V, and Lindroos [20] assumed it to be a background star based on photometric color and brightness. However, Gahm et al. [16] attributed it to young stars due to the presence of H, KCaII and Hβ emission lines in this component, which are attributed to young stars. Also, an interesting point is that the projection of the disk of the component A onto the line AB is about halfway along the line. The study of the spectrum of this three-fold system in the visual field can allow us to make an opinion about the dynamics of the system.

Based on photometric and spectral observations, Weinberger et al. [21] showed that HD141569 forms a triple system. The spectral classes of D and C components are assigned as M2 and M4, respectively. A characteristic Hα emission line and TiO bands were observed in the spectra of both components.

In this work, the results of spectral observations of the HD141569 star at the Shamakhi Astrophysical Observatory in 2017-2018 are given.

2. OBSERVATION MATERIAL

Observations in 2017-2018 carried out using the ShAO Fiber-Echelle Spectrograph (ShAFES), developed jointly by specialists from ShAO and SAO. A detailed description of the technical characteristics of this spectrograph is given in [22]. A CCD STA4150A (USA) with a size of 4096×4096 px, with a pixel size of $15\,\mu$m, was used. The CCD cooled to a temperature of -120°C using liquid nitrogen. Spectral range $\lambda 3700 - 8000$. Observations were performed with a combination of 2×2 pixels (binning), which allows to obtain a spectral resolution of R = 28000.

As mentioned above, HD141569 is a dense triple system, with the B component 7.5 arcsec and the C component 1.5 arcsec from the central star. It was not possible to observe the components individually for two reasons: a) the brightness of the central component A is 6.88 mag in the J band, the brightness of the component B is 9.2mag, and the brightness of the component C is 10.16mag [21], b) the size of the image during the observation is $2 - 4$ arcsec, as a result of which the components cannot be distinguished in the image taken in the slit plane of the spectrograph. Therefore, although the received spectra have a share of emission from other components included in the triplet, the main emission is from the brighter component A.

A total of 8 pairs of spectra were obtained during the indicated period. The resulting pair of spectra were averaged for each night and subjected to the necessary processing at all initial stages. The acquired spectra were transferred to $*.200$ vector format and measurements were made. All processing and measurement procedures were performed in the DECH package (Galazutdinov G., http://www.gazinur.com/DECH-software.html). Table 1 provides basic information about the observation. In Table 1, columns from left to right show date of observation, Julian date, identification number of night-averaged spectrum, signal-to-noise ratio, universal time UT, and exposition time in seconds.

In each observation, the spectra of the object and standard stars were obtained. The errors obtained in the measurements are 4-5% in equivalent widths and 0.5% in intensities. In radial velocities it is ± 1.0 km/s. In this work, 2 pairs of spectra of the star obtained in 2017 and 6 pairs obtained in 2018 were studied.

Table 1. Journal of spectral observations of the star HD141569.

Observation dates	JD 2450000+	Mr	S /N	UT	Exp. time
20.05 .2017	7894.371	KF1011-12	100	20 : 54	3000
06.06 .2017	7911.2305	KF1046-47	100	17 : 32	2400
02.05 .2018	8240.5472	KF2245	100	01 : 08	2400
22.05 .2018	8260.5833	KF2395-96	100	02 : 00	2400
25.05 .2018	8264.2451	KF2447-48	100	17 : 53	2400
06.06 .2018	8276.2417	KF2457-58	100	17 : 48	2400
07.06 .2018	8277.2256	KF2880-81	100	17 : 25	2400
27.06 .2018	8297.2312	KF2644-45	100	17 : 33	2400

3. HYDROGEN LINES-Hα.

The measured spectrophotometric parameters of the Hα line are also given in Table 2 consists of two parts. In the first part, from left to right, JD dates, the equivalent width of the blue absorption component EWa1, the equivalent width of the emission component EWe, the equivalent width in the red wing absorption EWa2, and the intensities of the blue absorption, blue emission, red emission, and red wing absorption components, respectively, Ia1, Ie1, Ie2, Ia2 are given. In the second part of table 2, the half-width FWHM of the emission component, the radiative velocities of the blue emission peak (RV1p), the red emission peak (RV2p), the bisector velocity (RVbis) and the central absorption of emission component radial velocities (RV_Ca) are given for the same JD dates. Figure 1 shows one of

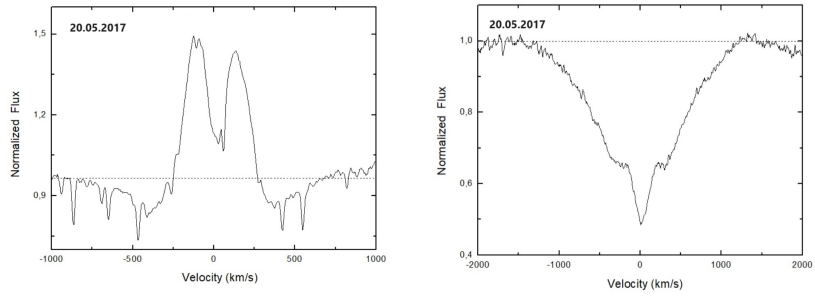

Fig. 1. Profiles of the lines Hα (left) and Hβ (right).

the typical profiles of the Hα line. As can be seen, the broad wings belonging to the A0V photosphere line and the emission component with a two-peak emission profile in the center of the line are clearly distinguished. In the profiles taken

Table 2. Obtained spectral parameters of selected components in the line Hα.

Date	E W a1 (Å)	E W e (Å)	EWa2 (Å)	Ia1	Ie1	Ie2	Ia2
20.05 .2017	2.01	2.64	1.3	0.18	-0.47	-0.16	0.39
06.06 .2017	2.6	1.85	1.93	0.25	-0.36	-0.25	0.34
02.05 .2018	2.04	3.35	1.38	0.26	-0.58	-0.22	0.55
22.05 .2018	2.58	2.45	1.59	0.24	-0.44	-0.35	0.21
25.05 .2018	1.91	2.7	1.08	0.3	-0.5	-0.39	0.26
06.06 .2018	2.13	2.88	0.98	0.23	-0.5	-0.45	0.2
07.06 .2018	1.78	3.04	1.01	0.26	-0.49	-0.44	0.23
27.06 .2018	3.23	2.65	1.39	0.28	-0.44	-0.41	0.24
Date	FWHM (Å)	RV1p (km/h)	RV2p (km/h)	RVbis (km/h)	RV Ca (km/h)		
20.05 .2017	8.21	-130	118	-4.11	1.61		
06.06 .2017	8.15	-134	122	6.91	-2.11		
02.05 .2018	8.27	-124	103	-0.76	-11.98		
22.05 .2018	8.08	-129	119	0.54	-7.38		
25.05 .2018	8.13	-137	107	-4.03	-15.7		
06.06 .2018	8.3	-130	112	-1.58	-1.58		
07.06 .2018	8.61	-125	133	3	8.61		
27.06 .2018	8.34	-122	135	0.32	3.37		

on different nights, the radial velocity and intensities of the components show obvious variations. At the same time, the materials obtained in 2017 and 2018 show that changes have occurred in the spectrum for a long time.

4. Hβ LINE

In the Hβ line profile, unlike Hα, the emission components are sharply weaker (Fig. 1, right panel). Therefore, it was not possible to measure the parameters of the emission components. Table 3 lists the parameters of the absorption profile of the Hβ line. Both the line profile and the smaller equivalent width compared to normal A0V stars indicate that the inner part of the line is distorted by the emission component. Table 3 shows that the bisector velocity of the Hβ line changed significantly in 2017 and 2018.

Table 3. Selected parameters of the line Hβ.

Date	EWa (Å)	Ie	FWHM(Å)	RVp (km/h)	Rxbis (km/h)
20.05 .2017	8.76	0.51	16.15	1.05	-6.21
06.06 .2017	8.29	0.51	15.63	0.46	-9.41
02.05 .2018	10.42	0.58	16.4	-13.33	-11.09
22.05 .2018	9.4	0.52	17.21	-7.57	-17.66
25.05 .2018	8.87	0.53	18.17	7.67	4.71
06.06 .2018	8.73	0.51	16.71	-8.43	-16.23
07.06 .2018	8.4	0.51	15.53	4.95	4.95
27.06 .2018	8.19	0.5	15.49	2.36	13.67

5. Hγ-Hε LINES.

The emission component is completely absent in the profiles of the Hγ and subsequent Hδ and Hε lines of the star. Figure 2 shows the Hγ and Hε line profiles as examples. No significant changes in profiles were detected during the observation period. Some selected parameters of the indicated lines were measured and

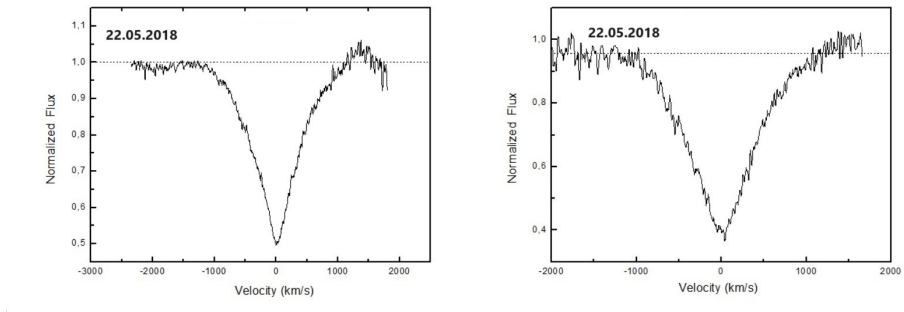

Fig. 2. Profiles of the lines $H\gamma$ (left) and Hε (right).

listed in Tables 4 and 5.

6. HEI AND D NAI LINES.

Table 6. the results of selected parameters of the lines HeI 5876. Designers of parameters the same as in other tables.

In the table designed of parametrs is the same as in other tables. In the table we see that relation of the the equivalent widts of lines D2/D1 is equal nearly 3:1. It is mean that this lines is formed in steallar atmosphere which normal termodinamic condition.

Table 4. Selected parameters of the line Hγ .

Date	EWa (Å)	Ie	FWHM (Å)	RVp (km/h)	R V bis (km/h)
20.05 .2017	5.93	0.5	10.76	-6.87	-27.49
06.06 .2017	6.4	0.5	11.43	-2.44	-15.34
02.05 .2018	7.9	0.59	11.77	-25.9	-12.53
22.05 .2018	7.03	0.52	11.64	-14.33	-25.68
25.05 .2018	6.47	0.51	12.45	-15.22	-24.6
06.06 .2018	7.1	0.53	11.59	-22.17	-34.88
07.06 .2018	6.27	0.5	10.83	-1.38	-4.88
27.06 .2018	7.88	0.53	13.09	-10.59	-14.18

Table 5. Selected parameters of the line Hε .

Date	EWa (Å)	Ie	FWHM (Å)	RVp (km/h)	RVbis (km/h)
20.05 .2017	6.7	0.56	10.42	4.53	-21.34
06.06 .2017	7.26	0.6	10.81	2.79	-21.42
02.05 .2018	7.04	0.57	11.03	4.8	2.24
22.05 .2018	7.11	0.6	10.67	-2.51	-2.51
25.05 .2018	7.49	0.62	11.04	-2.93	-32.76
06.06 .2018	7.81	0.61	11.44	-1.24	11.79
07.06 .2018	8.01	0.62	11.38	3.54	-15.75
27.06 .2018	8.26	0.6	12	4.92	1.29

Table 6. Parameters of the line HeI 5876.

Date	EW	Ie	FWHM	Rvp	Rxbis
20.05 .2017	0.04	0.04	0.94	28.76	27.16
06.06 .2017	0.13	0.07	1.45	20.67	13.26
02.05 .2018	0.29	0.07	4.85	10.52	10.52
22.05 .2018	0.2	0.04	2.47	-12.77	33.29
25.05 .2018	0.19	0.06	4.21	-7.28	8.99
06.06 .2018	0.05	0.03	1.13	-9.5	6.24
07.06 .2018	0.29	0.08	4.54	-21.66	-1.88
27.06 .2018	0.05	0.02	1.16	-21.57	-25.21

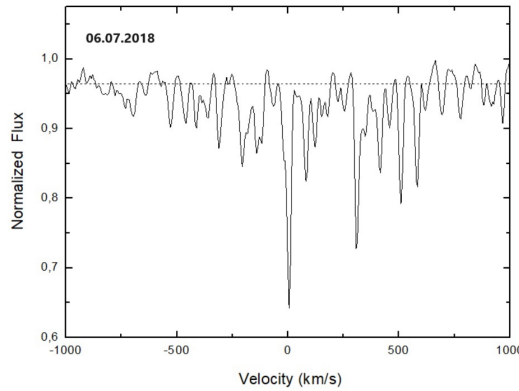

Fig. 3. Profiles of the lines D1, D2 NaI

Table 7. Selected parameters D1, D2 NaI lines

Date (D2)	EWa	I	FWHM	RVp	RVbis
20.05 .2017	0.18	0.35	0.43	-14.84	-14.84
06.06 .2017	0.32	0.39	0.56	-14.39	-14.39
02.05 .2018	0.72	0.45	1.44	-13.05	-13.05
22.05 .2018	0.28	0.37	0.44	-16.47	-16.47
25.05 .2018	0.43	0.4	0.53	-14.49	-14.49
06.06 .2018	0.49	0.33	0.47	-15.59	-15.59
07.06 .2018	1.54	0.34	0.48	-13.34	-14.46
27.06 .2018	0.5	0.33	0.48	-13.13	-13.13
Date(D1)	EWa	I	FWHM	RVp	RVbis
20.05 .2017	0.11	0.26	0.36	-14.14	-14.14
06.06 .2017	0.13	0.28	0.45	-13.03	-13.03

7. GENERAL SPECTRAL CHANGES

The emission components observed in the Hα line are symmetrically redshifted from the center of the line by about 120 ± 10 km/s, respectively. The central intensities of both components show little variation (Table 2). Figure 4 shows the graphs of the total equivalent width of the Hα emission line and the bisector radial velocity over time during the year 2018 . As can be seen from the graphs, the equivalent width of the emission line varies around the average value of 2.6 with a deviation of approximately ± 1. The bisector radial velocity varies around the mean value of 0 with a deviation of ± 3 km/s. Steinmetz et al. [23] $+3.5$ km/s,

Gontcharov [24] −6.4 km/s for the velocity of the star's mass center. As can be seen, the bisector radial velocity of the emission line is in good agreement with the velocity of the center of mass. The radial velocities of the other lines also show small variations around values corresponding to the velocity of the center of mass.

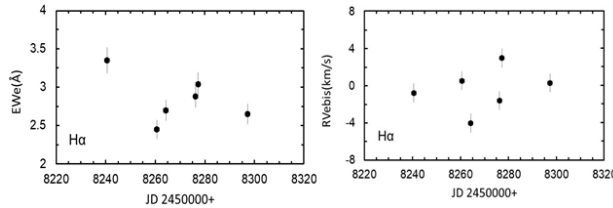

Fig. 4. Time variation of $H\alpha$ emission line equivalent width and bisector radial velocity during 2028.

Figure 5 shows the changes in time of the equivalent widths of the Hô photosphere line, free of the emission component, according to the observations made in 2027-2028, and the time changes of the radial velocity obtained in 2018. It can be seen from the figure that in 2017-2018 the equivalent widths show a change of up to 3. From the right panel of Figure 5, it can be seen that the maximum change in the bisector radial velocity due to the vary in intensity in the wings of the $H\delta$ line in 2018 alone is 25 km/s. It should be noted that similar variations in the spectrum of the star are also manifested in other spectral lines.

Figure 5. Variation of the equivalent width of the Hδ line over time in 2017-2018 (left panel). The right panel shows the change in the bisector radial velocity only in 2018.

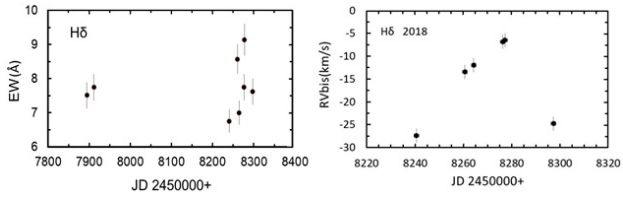

Fig. 5. Variation of the equivalent width of the Hδ line over time in 2017-2018 (left panel). The right panel shows the change in the bisector radial velocity only in 2018.

8. DISCUSSION AND CONCLUSIONS

This, the spectrum of the HD141569 star obtained in 2017 and 2018 were compared and it was shown that certain variations in the spectrophotometric parameters of the lines were detected during this period. It should be noted that despite the star's luminosity being $V = 7mag$, its optical spectrum has not been extensively studied. Most of the articles written in a large number are devoted to the structure of the circumstellar disk and the issues of planet formation in the disk. Herman and Duval [25] first showed that the H line has a two-peaked emission and central absorption profile, and the equivalent width of this line varies in the range of $2 - 5$. These authors determined the distance between the peaks to be 2.5 (114 km/s). Hubert Delplas and Hubert [26], summarizing the material obtained over 12 years, showed that the emission lines in the spectrum of this Be-type star do not varied.

The intensity of the emission component in the Hα line is much stronger than in other lines of the Balmer series. The emission appears only in a weak form in the Hβ line. This means that the Balmer decrement can be maximally overestimated in the radiation from the disk. Such emission can be excited in gases only by electrons photons and that are not transparent to the Layman series. The mechanism of the generation of such high-energy particles in the circumstellar disk requires additional investigation.

The results obtained in this study showed that there are small changes in the emission spectrum of the star. This may be due to various variations occurring in the invariant disk, including accretion and stellar wind. The features in its spectrum indicate that HD141569 is a young star with a fragmented protoplanetary debris disk and may belong to the class of β Pictype stars.

REFERENCES

1. Beuzit, JL, Vigan, A., Mouillet, D., et al. 2019, A&A, **631**, A155

2. ALMA Partnership (Fomalont, EB, et al.) 2015, ApJ, **808**, L1

3. Lodato, G., Dipierro, G., Ragusa, E., et al. 2019, MNRAS, **486**, 453

4. Benisty, M., Stolker, T., Pohl, A., et al. 2017, A&A, **597**, A42

5. Augereau, JC, & Papaloizou, JCB 2004, A&A, **414**, 1153

6. Vioque, M., Oudmaijer, RD, Baines, D., Mendigutía, I., & Pérez-Martínez, R. 2018, A&A, **620**, A128

7. Di Folco, E., Péricaud, J., Dutrey, A., et al. 2020, A&A, **635**, A94

8. Arun, R., Mathew, B., Manoj, P., et al. 2019, AJ, **157**, 159

9. Meeus, G., Waters, LBFM, Bouwman, J., et al. 2001, A&A, **365**, 476

10. Currie, T., Grady, CA, Cloutier, R., et al. 2016, ApJ, **819**, L26

11. Biller, BA, Liu, MC, Rice, K., et al. 2015, MNRAS, **450**, 4446

12. Merín, B., Montesinos, B., Eiroa, C., et al. 2004, A&A, **419**, 301

13. Hillenbrand, LA, Strom, SE, Vrba, FJ, & Keene, J. 1992, Ap.J., **397**, 613

14. Mendigutía, I., Eiroa, C., Montesinos, B., et al. 2011, A&A, **529**, A34

15. Eisner, JA, Rieke, GH, Rieke, MJ, et al. 2015, MNRAS, **447**, 202

16. Gahm, GF ; Ahlin, P.; Lindroos, KP A & AS, Vol. 51, p. 143-159 (1983)

17. Herbig, GH 1960, ApJS,**4**, 337

18. The, PS, de Winter, D., & Perez, MR 1994, A&AS, **104**, 315

19. Rossiter, R. A. 1943, Publ. Michigan Obs., **8**, 133

20. Lindroos, KP 1985, A&AS, **60**, 183

21. Weinberger AJ, Rich RM, Becklin EE, Zuckerman B, Matthews K. 2000, Ap.J,. **544**, 937.

22. Mikailov Kh. M., Musaev FA, Alekberova IA, Rustamov BN, Khalilov OV, Kinematics and Physics of Celestial Bodies, 2020, **36**, No. 1, 22.

23. Steinmetz M., Guiglion G., Mcmillan PJ, et al. 2020 AJ.,**160**, 83S

24. Gontcharov GA 2006 Astron.Letters **32**, 759G

25. Herman R., Duval M. , 1962 , Ann. Astrophys. **25**, 9.

26. Hubert Delplas AM, and Hubert H: 1979, An atlas of Be stars. Paris. Meudon Observatory.